Effect of Steel Wool and Graphite on the Electrical Conductivity and Pavement Properties of Asphalt Mixture

Hanwen Yang, Jian Ouyang, Peng Cao, Wen Chen, Baoguo Han, Jinping Ou

Effect of Steel Wool and Graphite on the Electrical Conductivity and Pavement Properties of Asphalt Mixture

Hanwen Yang[1]; Jian Ouyang[2]; Peng Cao[3]; Wen Chen[4]; Baoguo Han[5]; and Jinping Ou[6]

Abstract: Electrically conductive asphalt mixtures (ECAM) were fabricated by adding two conductive materials (steel wool and graphite) in this paper. Effects of steel wool and graphite on the electrical conductivity and pavement properties of ECAM were studied. Results showed that steel wool can greatly reduce the electrical resistivity of asphalt mixtures. Meanwhile, ECAM with steel wool has an excellent low-temperature cracking resistance and a good moisture susceptibility and rutting resistance compared with the plain asphalt mixture. However, the aggregation problem of steel wool cannot be avoided at its high content. As a result, there is an upper limit of the content of steel wool. Graphite can not only effectively decrease the electrical resistivity of asphalt mixture but also has a good rutting resistance, and it can be easily dispersed in the mixture. To fabricate a uniform ECAM with better electrical conductivity and pavement properties, the hybrid addition of steel wool and graphite is employed. This method can reduce the steel wool content, thus solving the dispersion problem and further improving the electrical conductivity and pavement properties of asphalt mixture. Therefore, the hybrid addition method is more suitable for fabricating conductive asphalt mixtures. **DOI: 10.1061/(ASCE)MT.1943-5533.0004105.**

Author keywords: Electrically conductive asphalt mixture (ECAM); Electrical resistivity; Pavement properties; Steel wool; Graphite.

Introduction

Recent improvements in demands of roads have led to extensive attention to intelligent transportation. Traditional pavement materials are gradually becoming unable to meet the needs of human beings. In an intelligent transportation system, the road should possess many intelligent properties to the vehicles and environment as well as itself such as self-sensing and self-healing, except for having enough carrying capacity to vehicles. A theoretically feasible way is to develop intelligent pavement materials, aiming to achieve these intelligent properties in road (Wang et al. 2019; Shen et al. 2020; Wu et al. 2015).

Intelligent pavement materials may be defined as the mixture of traditional pavement materials and functional components to improve the nonmechanical properties, such as electrical, thermal, and acoustic properties. Some types of functional pavement are proposed by utilizing these nonmechanical properties, such as self-sensing pavement (Han et al. 2013; Xin et al. 2020), self-healing pavement (Norambuena-Contreras and Garcia 2016; Norambuena-Contreras et al. 2018; Li et al. 2020a), self-melting snow pavement (Zhang et al. 2016; Rao et al. 2018), self-powered pavement (Hasni et al. 2017), noise-reduction pavement (Faßbender and Oeser 2020), and piezoelectric pavement (Na and Baek 2019; Na 2019), among others. Among these functional pavements, most of them are highly dependent on the electrically conductive properties of pavement materials. The following examples are used to illustrate this point: (1) self-sensing pavements have typically relied on the relation between the electrical resistivity and strain of the material; and (2) the self-healing pavement is based on microwave heating and induction heating technology, whose heating efficiencies are highly related to the electrical conductivity of pavement materials. Therefore, fabrication of asphalt mixtures with high electrical conductivity plays a crucial role in the research of functional pavements.

It is well-known that a plain asphalt mixture is an insulated material (Ha et al. 2019), and electrically conductive materials (ECMs) are normally added to improve the electrical conductivity of asphalt mixtures. In some previous studies about electrically conductive asphalt mixtures (ECAMs), it has been demonstrated that some ECMs can be used to fabricate the ECAM to improve the electrical conductivity of asphalt mixtures, such as carbon nanotubes (Ameri et al. 2016), graphene (Moreno-Navarro et al. 2018), carbon black (Ou and Han 2009), carbon fibers (Wang et al. 2016), graphite (Wu et al. 2003), magnetic metals (Ye et al. 2019), nickel powder (Han et al. 2009), steel fibers (García et al. 2009), and steel wool (Norambuena-Contreras and Garcia 2016). These materials can be divided into three types: nano-level materials, micrometer-level materials, and centimeter-level materials.

For nanomaterials like graphene, the rheological properties and thermal sensitivity tests proved that graphene was beneficial to the mechanical and thermal properties of asphalt binder (Moreno-Navarro et al. 2018). However, because of the strong van der Waals forces in graphene molecules, dispersion of graphene is a critical issue, especially at a relative high content of graphene. Besides, its high price can also limit its application in pavement materials. Micrometer material–modified asphalt mixtures, such as graphite-modified asphalt composites, can have a self-sensing ability of strain, defects, and temperature through the change of electrical resistance (Wu et al. 2003). However, due to the lubrication

[1]Ph.D. Candidate, School of Civil Engineering, Dalian Univ. of Technology, Dalian 116024, China. Email: hanwen_yang1103@126.com

[2]Associate Professor, School of Transportation and Logistics, Dalian Univ. of Technology, Dalian 116024, China (corresponding author). ORCID: https://orcid.org/0000-0003-4673-6171. Email: ouyangjian87@126.com; ouyangjian@dlut.edu.cn

[3]Associate Professor, College of Architecture and Civil Engineering, Beijing Univ. of Technology, Beijing 100124, China.

[4]Associate Professor, Laboratoire d'Etude des Microstructures et de Mecanique des Materiaux, Universite de Lorraine, Nancy 54000, France.

[5]Professor, School of Civil Engineering, Dalian Univ. of Technology, Dalian 116024, China.

[6]Professor, Dept. of Civil Engineering, Dalian Univ. of Technology, Dalian 116024, China.

Note. This manuscript was submitted on March 19, 2021; approved on July 1, 2021; published online on December 21, 2021. Discussion period open until May 21, 2022; separate discussions must be submitted for individual papers. This paper is part of the ***Journal of Materials in Civil Engineering***, © ASCE, ISSN 0899-1561.

properties of graphite, the increase of graphite content can decreased the mechanical properties of the mixture. Centimeter material–modified asphalt mixtures, such as steel wool–modified asphalt mixtures, can have good electrical conductivity. Thus, the steel wool–modified asphalt mixture possess a self-healing ability by a microwave heating and induction heating device. Based on the preceding analysis, the dispersion of the highly electrically conductive materials, the price of the ECMs, and mechanical properties of ECAMs are the mainly problems that need to be solved. The interface diagram and actual adhesion state of steel wool and asphalt mastic is shown in Fig. 1.

It is remarkable that the interface bond properties between steel wool and asphalt mastic are weak, which is similar to that of steel fibers (Guo et al. 2020). Because of the weak adhesion between steel wool and asphalt mastic, the connected conductive networks that may create some open circuits in small areas in the mixture cannot form, which can have a negative effect on the local electrical conductivity of the ECAM. Although the graphite can be well-dispersed on the ECAM to ensure the global and local electrical conductivity of the ECAM, it exhibits a harmful impact on some mechanical properties. Hence, the electrical conductivity and mechanical properties may not be satisfied simultaneously by the single addition method.

The novelty and practical application of this work is to fabricate a pavement material with good electrical conductivity and pavement properties. Based on the good electrical conductivity, the asphalt mixture can be easily heated through induction heating devices. Besides, this novel pavement material should also have better pavement properties to ensure its higher durability compared with traditional pavement materials. Therefore, two kinds of relatively cheaper and conductive materials (graphite and steel wool) at the micrometer and centimeter levels were blended into the asphalt mixture to fabricate intelligent pavement materials with better electrical conductivity and pavement properties. Besides, the form of steel wool is fiber; thus, the electrical conductivity of steel wool is mainly determined by its aspect ratio, and the electrical conductivity of graphite is affected by its geometry because the form of graphite is powder. Therefore, steel wool with three diameters and flake graphite were used as conductive materials, and three kinds of ECAMs with single and hybrid ECMs were studied to give full play to the advantages of materials.

A comprehensive laboratory testing program was used to evaluate the electrical conductivity and pavement properties of ECAMs for determining the optimal amount of ECMs. The laboratory testing program was performed in two stages. In the first stage, the optimal proportions of ECMs for the three ECAMs were determined by electrical resistivity. Furthermore, the effect of different ECMs on the electrical conductivity of ECAMs was discussed. In the second stage, the water sensitivity and high- and low-temperature performances of the three ECAMs at the optimum mix were evaluated. Meanwhile, their pavement properties were compared with a plain asphalt mixture. The framework of the research is shown in Fig. 2.

Experimental Program

Materials

The raw materials in ECAM include limestone aggregate, limestone powder, asphalt, steel wool, and graphite. The steel wool, as a fiber, was acquired from Ezhou Baofeng Metal Wool Technology (Ezhou, China). Approximately 3,000 t of steel wool is produced every year in this manufacturing factory. There are many factories that can produce steel wool in the world; thus, the availability of steel wool is sufficient. Graphite, as a powder, was acquired from Qinghe Yuanyao Alloy Products (Xingtai, China). The densities of limestone aggregate, limestone powder, asphalt, steel wool, and graphite are 2.71, 2.77, 1.02, 7.2, and 2.1 g/cm^3, respectively. Three types of steel wool with different diameters (named as Nos. 4, 2, and 0) and one type of graphite were used in the experiment, with their chemical, physical properties, and prices listed in Table 1.

Compared with some common conductive materials, like carbon nanotubes ($0.10/g), graphene ($0.23/g), carbon fiber ($0.03/g), nickel powder ($0.02/g), steel wool ($0.005/g), and graphite ($0.007/g) are cheaper than those electrically conductive materials. The three types of steel wool have the same basic properties except diameter. The morphology of steel wool and the particle-size distribution of graphite and limestone powder are shown in Fig. 3. The basic properties of asphalt are given in Table 2 (China DOT 2011). A uniform dense aggregate gradation for AC-13 was used in this study according to the Chinese technical specification (China DOT 2011). Fig. 4 presents the gradation of design gradation and specification limits.

Three types of the ECAMs were fabricated, which are an asphalt mixture with pure steel wool, an asphalt mixture with pure graphite, and an asphalt mixture with both steel wool and graphite, respectively. Their names are recorded as ECAM-S, ECAM-G, and ECAM-SG. ECAM-Ss with four contents of steel wool (i.e., 2%, 4%, 6%, and 8% by the volume fraction of asphalt) were fabricated. For ECAM-S with various contents of steel wool, three types of steel wool (Nos. 4, 2, and 0) were considered. ECAM-Gs with four contents of graphite (i.e., 10%, 12%, 15%, and 20% by the volume fraction of asphalt) were also fabricated. The optimum content of steel wool and graphite for ECAM-SG is determined from ECAM-S and ECAM-G. Meanwhile, the plain asphalt mixture served as the control group, and its name is recorded as AM.

Specimen Preparation

The Marshall design method was used to determine the optimum asphalt content of mixtures according to JTG F40-2004 (China DOT 2004). Because the oil absorption ratio of graphite differs from that of limestone powder, asphalt mixture with different

Fig. 1. (a) Interface diagram; (b) adhesion state under mixing; and (c) adhesion state under compaction.

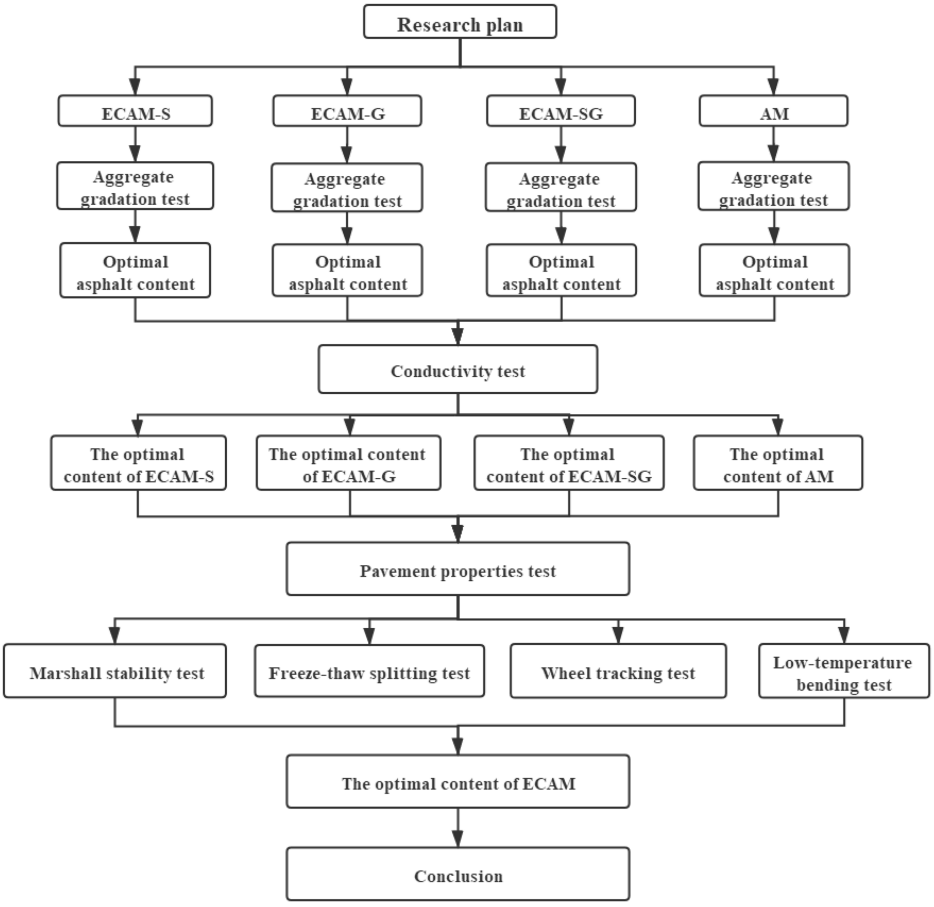

Fig. 2. Framework of the research.

Table 1. Basic information of steel wool and graphite

Type	Property	Value	Type	Property	Value
Steel wool	No. 4 diameter	0.1 mm	Graphite	Shore hardness	40–45
	No. 2 diameter	0.075 mm		Specific gravity	1.9–2.3
	No. 0 diameter	0.05 mm		Melting point	$\leq$ 3,000°C
	Length	4 mm		Boron concentration	$\geq$ 0.5 ppm
	Shape	Velvet		Particle size	30–50 μm
	Steel content	99.86%		Shape	Flaky
	Chemical composition	Cd, Pb, Hg, Cr(VI)		Fixed carbon content	99.90%
Price		\$0.005/g	Price		\$0.007/g

graphite contents can have different optimal asphalt contents. The optimal asphalt content of asphalt mixtures with different graphite contents is calculated according to Eq. (1) (Li et al. 2017)

$$P_a = \frac{S \times K \times a}{100} + M \tag{1}$$

where P_a = optimal asphalt content; S = mass ratio of graphite to the replacement of limestone powder; K = mass ratio of limestone powder to all aggregates; a = difference of oil absorption ratio; and M = optimal asphalt content of asphalt mixture without graphite. The oil absorption ratio of graphite is 0.5% higher than that of limestone powder (Li et al. 2017); thus, a in Eq. (1) is 0.5. Besides, in a previous study, the difference of the optimal asphalt content between 2% and 4% by volume of steel wool with the same length is just 0.03%. Thus, it is assumed that the optimal asphalt content of different steel wool and graphite contents only depend on the contents of graphite in this paper. According to Eq. (1), the optimal asphalt contents of asphalt mixture with different graphite contents are summarized in Table 3.

The specimens were prepared according to the aggregate gradation and optimal asphalt content of the mixture. The process of the preparing the ECAM is similar to that of the plain asphalt mixture, and the steel wool does not need to be treated before the test. First, the aggregates, asphalt, and limestone powder were preheated to the mixing temperature of 160°C. Aggregates and steel wool were firstly added into a blender and mixed for 90 s. Then, asphalt was added for the following 60 s mixing. Finally, graphite and limestone powder were added and mixed for 30 s. The only difference in the aforementioned operation is the handling process of steel wool. In order to avoid the agglomeration of steel wool, the steel wool should be screened by a 4.75-mm mesh sieve before adding to

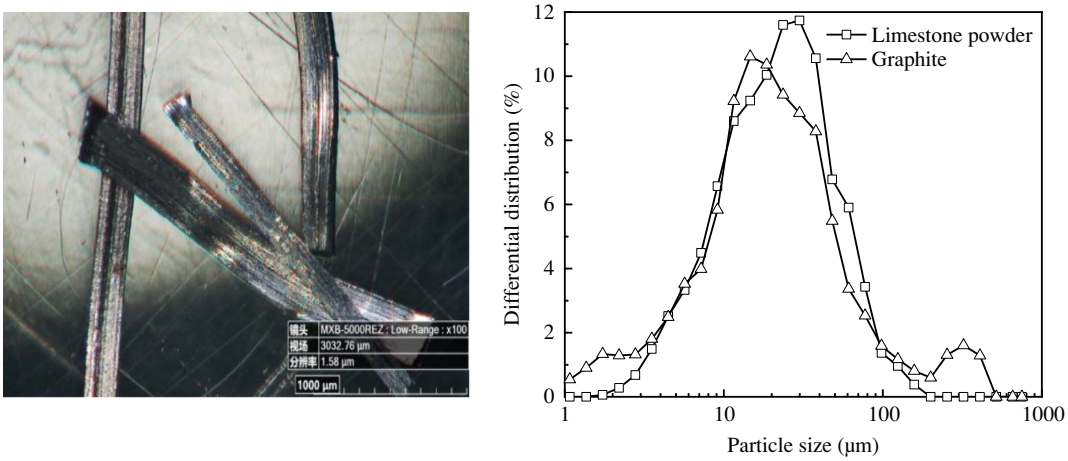

Fig. 3. (a) Morphology of steel wool; and (b) particle-size distribution of graphite and limestone powder.

Table 2. Basic properties of asphalt

Properties	Penetration, 25°C, 100 g (0.1 mm)	Softening point (°C)	Ductility, 15°C (cm)
Value	87.0	46.0	>150
Method	T0604	T0606	T0605

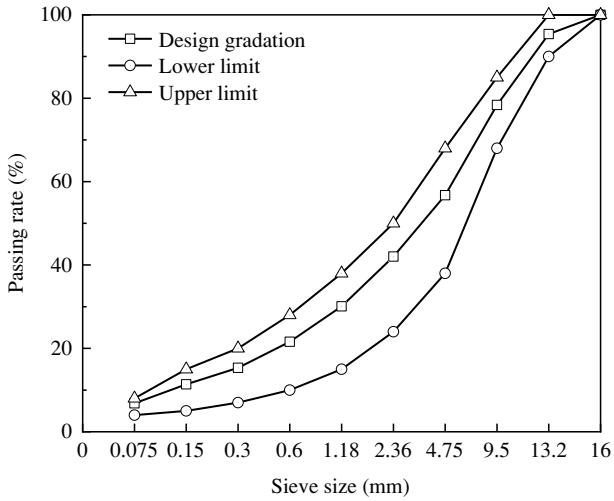

Fig. 4. Gradation of ECAM.

Table 3. Optimal asphalt content with different graphite contents of asphalt mixtures

Graphite content (% by volume)	Optimal asphalt content (%)
0	4.7
10	5.18
12	5.30
15	5.41
20	5.52

the mixture. At least three specimens were prepared for each type of ECAM in all tests.

Testing Program

Conductivity Test

Generally, the electrical conductivity of a mixture can directly affect its thermal conductivity, as shown in Eq. (2) (Jolliffe et al. 1966). The thermal conductivity is inversely proportional to electrical resistivity, so a lower electrical resistivity of a mixture is greatly beneficial to increasing the temperature of a mixture during the application of the microwave or induction heating technology. Therefore, the conductivity test was done based on this objective

$$\lambda = 2.7 \times 10^{-8} T/\rho \tag{2}$$

where λ = thermal conductivity of the mixture; T = absolute temperature; and ρ = electrical resistivity of mixture.

The resistivity of an asphalt mixture is usually measured by two-point and four-point methods. The four-point method needs to embed electrodes in specimens, which is very difficult to operate in an asphalt mixture. Thus, the resistivity of ECAM is measured by the two-point method. A Keithley 2100 Digit Multimeter (Keithly, Cleveland) was used in this test. The specific operation processes are as follows. Firstly, as shown in Figs. 5(a and b), the electrodes were placed onto the specimen in the order of copper electrode, graphite layer, specimen, graphite layer, copper electrode. Graphite powder was used to fill the gaps between the electrodes and specimens to ensure a perfect contact between them. Secondly, as shown in Fig. 5(c), the probes of the multimeter were placed on the upper and lower copper electrodes. Then, the resistance data of the specimen were recorded when the value was stable. Each specimen was needed to test resistance values at four different places, and the average value was taken as the resistance value of each specimen. Finally, the electrical resistivity was calculated by the measured resistance according to Eq. (3)

$$\rho = \frac{R \cdot L}{S} \tag{3}$$

where ρ = resistivity of the specimen (Ω m); R = resistance of the specimen (Ω); L = diameter of the specimen (m); and S = cross-sectional area of the specimen (m^2).

(a) (b) (c)

Fig. 5. (a) Graphite layer; (b) placement sequence of the specimen; and (c) position of the probes of the multimeter.

Pavement Properties Test

Moisture Susceptibility

Moisture susceptibility was evaluated by both Marshall immersion test and freeze–thaw splitting test according to the Chinese specification (China DOT 2011). Two groups with eight specimens were tested in the Marshall immersion test. The first and second groups of specimens were prepared for common and immersed Marshall stability tests, respectively. The four specimens used in the common Marshall stability test were submerged in 60°C for 30 min, and the other specimens were submerged in 60°C for 48 h. The residual Marshall stability was calculated by using Eq. (4)

$$\text{RMS} = \frac{MS_1}{MS} \times 100 \tag{4}$$

where RMS = residual Marshall stability (%); and MS_1 and MS = average value of Marshall stability in the second and first groups, respectively.

The freeze–thaw splitting test was similar to the Marshall stability test. The specimens of the first group were submerged into water at 25°C for 2 h before testing. The treatment processes of the specimens in the second group were as follows: (1) the specimens were saturated for 15 min in the water bath under the vacuum condition with a pressure of 97.3–98.7 kPa; (2) the air pressure was recovered to normal condition, and then the specimens were continually submerged in the water bath for 30 min; (3) the specimens were placed in the chamber at −18°C for 16 h, and then put in the thermostatic tank with 60°C immediately; and (4) the specimens were finally submerged into water at 25°C for at least 2 h. The loading rate and test temperature of all specimens were 50 mm/min and 25°C in the splitting test, respectively. The freeze–thaw splitting tensile strength ratio (TSR) can be determined by applying Eq. (5)

$$\text{TSR} = \frac{\bar{R}_{T2}}{\bar{R}_{T1}} \times 100 \tag{5}$$

where TSR = freeze–thaw splitting tensile strength ratio (%); and $\bar{R}_{T1}$ and $\bar{R}_{T2}$ = average splitting tensile strength of specimens in the first and second groups (MPa), respectively.

Wheel Tracking Test

Wheel tracking testing was to evaluate the rutting resistance of asphalt mixtures at high temperature. The specimens with dimension 300 × 300 × 50 mm were placed in a dry condition at 60°C for 6 h. The walking distance of the test wheel was 230 mm, and the rolling speed was 42 cycles/min. A LVDT was used to measure the vertical displacement of specimens. The dynamic stability of the ECAM was calculated as an index of rutting resistance according to the Eq. (6)

$$DS = \frac{(t_{60} - t_{45}) \times N}{d_{60} - d_{45}} \tag{6}$$

where DS = dynamic stability; t_{60} and t_{45} = rutting time at 60 and 45 min, respectively; N = wheel traveling ($N = 42$ cycles/min); and d_{60} and d_{45} = rutting depth at 60 and 45 min, respectively.

Low-Temperature Beam Bending Test

Low-temperature beam bending testing was used to evaluate the cracking resistance of asphalt mixtures under low temperature. The specimens with dimensions $(250 \pm 2) \times (30 \pm 2) \times (35 \pm 2)$mm were placed in the chamber at −10°C for at least 4 h before testing. The test was conducted by a UTM-100 (IPC, Boronia, Australia) at −10°C with a constant deformation rate of 50 mm/min. The peak load at failure and the vertical deflection of the beam center were recorded. According to the deformation and vertical deflection, the bending tensile strength and failure strain were calculated based on the following equations:

$$R_B = \frac{3 \times L \times P_B}{2 \times b \times h^2} \tag{7}$$

$$\varepsilon_B = \frac{6 \times h \times d}{L^2} \tag{8}$$

where R_B = bending tensile strength of the specimen; ε_B = failure strain; L = beam length between the two support points; P_B = maximum load; b and h = width and height of the specimen, respectively; and d = midspan deflection under failure.

Electrical Conductivity of ECAM

Effect of Types and Contents of Steel Wool

The effects of types and contents of steel wool on the electrical conductivity of ECAM-S are displayed in Fig. 6. For all ECAM-S with the three types of steel wool, the electrical resistivity of ECAM-S decreases greatly with steel wool content from 0% to 6%, and then it decreases slowly with the continuous increment of steel wool content. It was observed that 6% is the optimum steel wool content for the electrical conductivity of all ECAM-S. It is worth noting that the fibers with smaller diameter are likely to be used in the asphalt mixture (i.e., a greater number of fibers per unit volume of asphalt mixture) to create more interconnected networks if the agglomeration phenomenon of steel wool does not happen in the mixture. Thus, the resistivity of the mixture should decrease with the decreasing diameters of the steel wool, but the electrical resistivity of ECAM-S at the same content of steel wool decreased a lot by increasing diameter of steel wool in the test. In other words, ECAM-S with No. 4 steel wool has the lowest electrical resistivity in this test, which is an abnormal phenomenon.

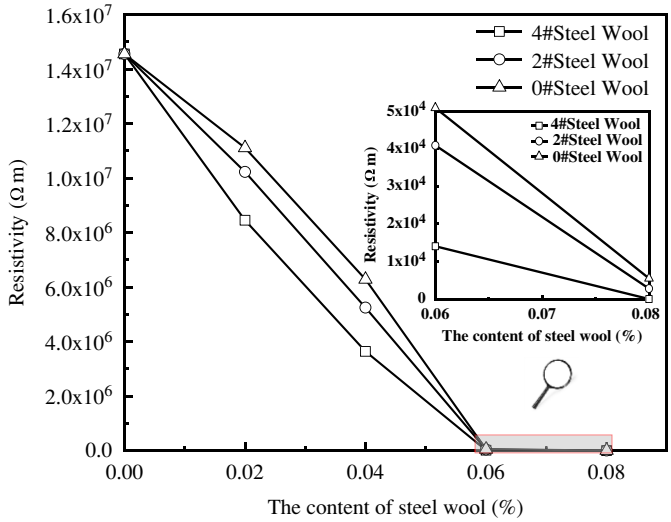

Fig. 6. Resistivity values of ECAM-S.

Consequently, there may be other reasons accounting for this phenomenon, which are discussed in the following paragraph.

To explain the abnormal phenomenon, the agglomeration phenomenon of steel wool is analyzed. Figs. 7–9 show the natural state, sieving state, and mixing state of three types of steel wool at the content of 4%. It can be seen from Figs. 7(a), 8(a), and 9(a) that the agglomeration phenomenon can be observed in Nos. 0 and 2 steel wool in the natural state, but No. 4 steel wool is well -ordered. Although the agglomeration phenomenon can be weakened after the steel wool is screened by the 4.75-mm mesh sieve [Figs. 7(b), 8(b), and 9(b)], this phenomenon can be still reappear after the steel wool is mixed with aggregates for Nos. 0 and 2 steel wool [Figs. 7(c), 8(c), and 9(c)].

Besides, the agglomeration phenomenon becomes more pronounced for steel wool with the smaller diameter [Figs. 7(c), 8(c), and 9(c)]. Perhaps the stiffness of steel wool decreases with the decreasing diameter so that its bending and torsional deformation are more notable during mixing. Thus, the effective conductive network of steel wool decreases for Nos. 0 and 2 steel wool imposed by the agglomeration phenomenon. This is why steel wool with a larger diameter (with a higher stiffness) is more easily dispersed in the mixture and the ECAM with No. 4 steel wool has a lowest resistivity compared with the ECAM with Nos. 2 and 0 steel wool.

In addition, the agglomeration phenomenon can easily lead to local circuit breaks in the mixture, resulting in an uneven electrical conductivity of the mixture. Therefore, if one uses the Nos. 0 and 2 steel wool to fabricate the ECAM or uses a higher content of steel wool, the electrical conductivity of the composite may be improved, but the agglomeration phenomenon of the steel wool can also appear in the mixture. Besides, this agglomeration phenomenon can directly cause uneven electrical conductivity of the ECAM. Especially in self-healing pavement, the uneven distribution of the electrically conductive materials will cause the local overheating and uneven temperature distribution, which is a big problem in the self-healing performance of asphalt mixtures in practical applications (Sun et al. 2017). Therefore, in consideration of the electrical conductivity and the agglomeration phenomenon, No. 4 steel wool is recommended to fabricate the ECAM.

Effect of Graphite Content

Effects of graphite content on the electrical conductivity of ECAM-G are shown in Fig. 10. It can be seen from Fig. 10 that the electrical resistivity of ECAM-G firstly decreases slightly with the increasing graphite content from 0% to 10%, then decreases

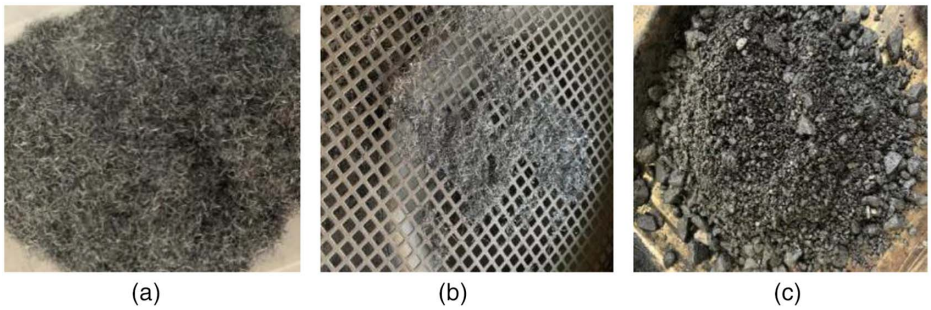

Fig. 7. (a) Natural state; (b) sieving state; and (c) mixing state of No. 4 steel wool.

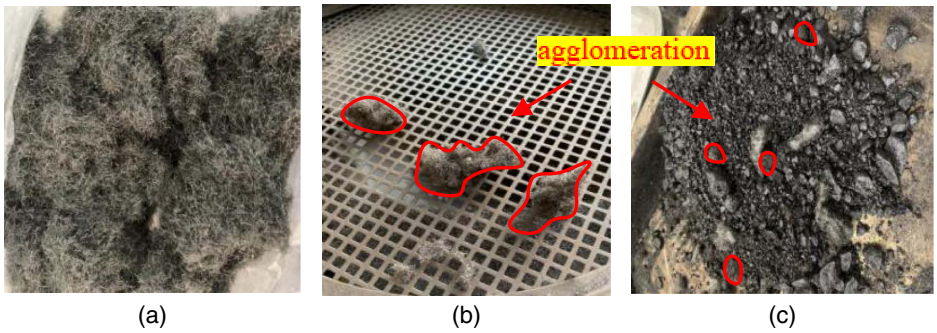

Fig. 8. (a) Natural state; (b) sieving state; and (c) mixing state of No. 2 steel wool.

J. Mater. Civ. Eng., 2022, 34(3): 04021466

Fig. 9. (a) Natural state; (b) sieving state; and (c) mixing state of No. 0 steel wool.

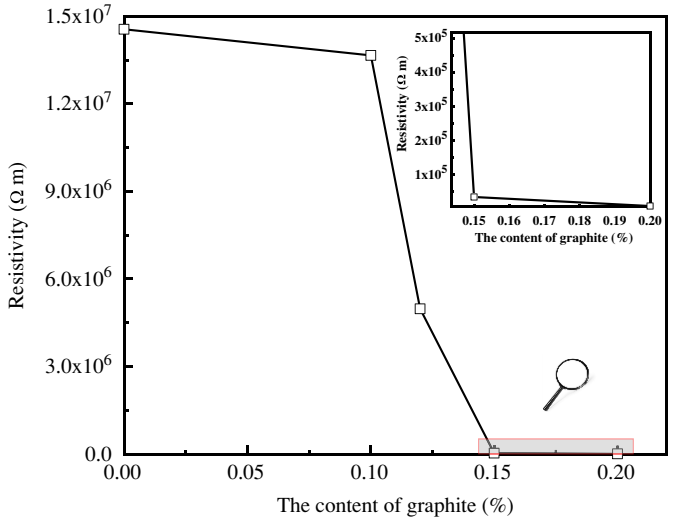

Fig. 10. Resistivity values of ECAM-G.

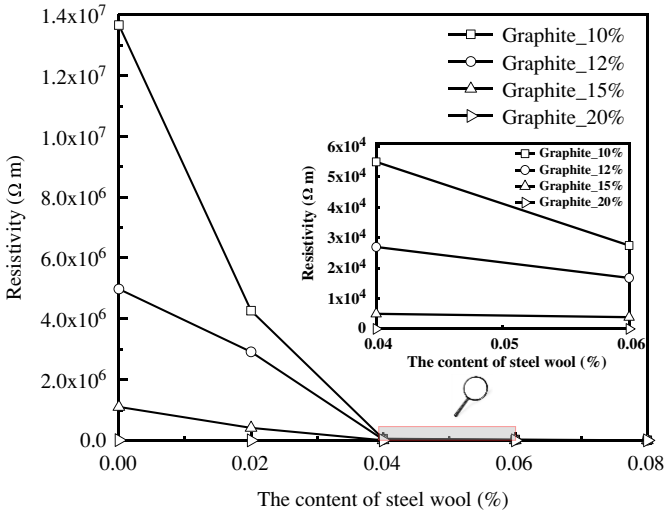

Fig. 11. Resistivity values of ECAM-SG.

sharply with the graphite content from 10% to 15%, and finally the downward trend levels off. The optimum graphite content of the electrical conductivity of ECAM-G is 15%. By comparison with Figs. 6 and 10, it can be seen that the trend of the electrical resistivity of ECAM with graphite content is significantly different from that with steel wool content, especially for low content. Differently from the ECAM-S, for lower graphite content, the resistivity of ECAM-G is similar to that of plain asphalt mixture, exhibiting insulating behavior. A sudden change in the resistivity takes place after a certain content of the graphite has been added. This difference between graphite and steel wool is primarily due to the fact that graphite is a conductive particle. When its content is much lower, no conductive network can be formed in the mixture. Thus, there is a notable seepage effect for ECAM-G, which the conductivity of composites suddenly increases by several orders of magnitude only when the volume fraction of conductive particles reaches a certain critical value. But for steel wool, its aspect ratio is very beneficial to form a conductive network so that no notable seepage effect can be observed for ECAM-S.

The electrical resistivity values of ECAM-S with No. 4 steel wool and ECAM-G at the optimum content are 14,047 and 33,457 Ω m, respectively. Definitively, ECAM-S with 6% No. 4 steel wool has a better electrical conductivity than ECAM-G with 15% graphite. However, as mentioned previously, the agglomeration phenomenon easily occurs during mixing, leading to an uneven electrical conductivity and poor mechanical properties of the composite. In our experiment, once the content of steel wool reaches 6%, the agglomeration phenomenon of ECAM-S with No. 4 steel wool is also pronounced during the mixing process. Thus, to ensure a uniform material, the steel wool content should be limited at 4%. On the contrary, graphite can be well dispersed on no matter how high its content; thus, the electrical conductivity of ECAM-G is better than that of ECAM-S from this point of view.

Effect of Hybrid Addition of Steel Wool and Graphite

As mentioned previously, adding a single conductive material to an asphalt mixture has certain limitations in improving the electrical conductivity of the asphalt mixture. Once the optimum contents of the steel wool and graphite have been reached, the electrical resistance of the ECAM-S and ECAM-G cannot decrease greatly no matter how much more content is used to fabricate the composite. Therefore, for fabricating a more highly electrically conductive composite, steel wool and graphite are both used to further improve the electrical conductivity of ECAM in this section. Considering that the electrical resistivity of ECAM-SG may be significantly different from that of ECAM-S and ECAM-G, the effect of steel wool content on the electrical resistivity of ECAM with different graphite content is studied, which is shown in Fig. 11. In this study, only No. 4 steel wool is utilized according to the preceding analysis of types of steel wool.

It has also been discovered from Fig. 11 that the electrical resistivity of all ECAM-SGs except ECAM-SG at 20% graphite

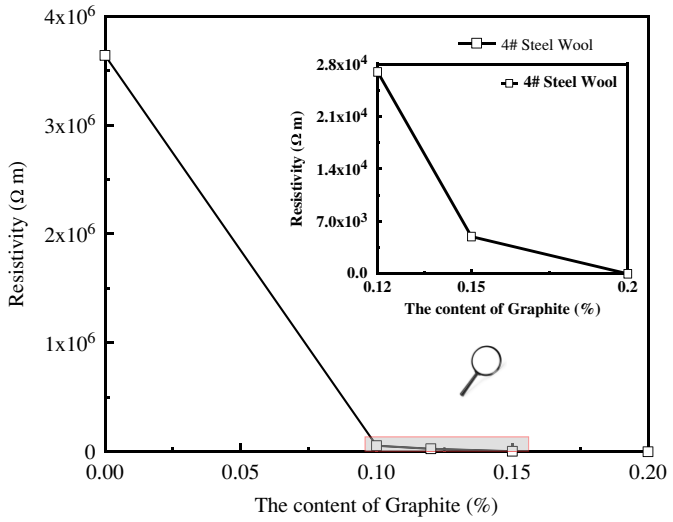

Fig. 12. Effect of graphite content on the electrical resistivity of ECAM with 4% steel wool.

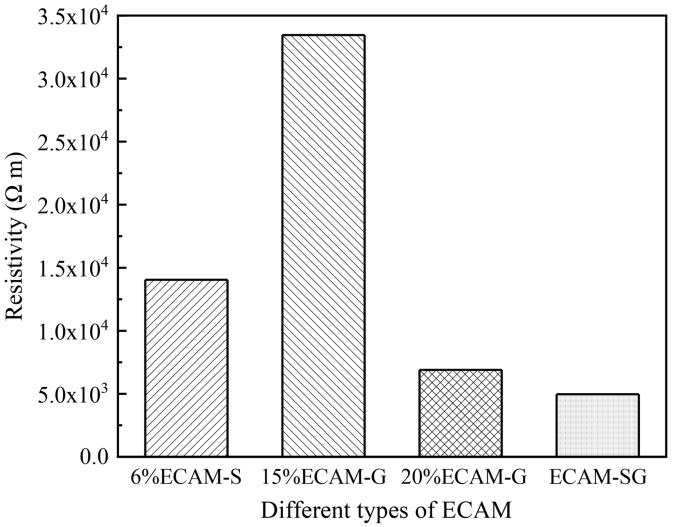

Fig. 13. Electrical resistivity values of different ECAMs.

firstly decreases quickly with the increasing steel wool content from 0% to 4% and then decreases very slowly with the continuous increment of steel wool content. ECAM-SG at 20% graphite has a relative good electrical conductivity no matter how high the content of steel wool is; thus, the addition of steel wool has no further effect on improving the electrical conductivity of ECAM-SG. In addition, the optimum steel wool content of ECAM-SG is 4%, which is lower than that of ECAM-S. This can be explained as follows. In the beginning, the steel wool is well distributed in the mixture, but the content of steel wool has a limit imposed by the agglomeration phenomenon; it is hard to form more conductive paths so that the electrical resistivity of the composite cannot decrease greatly. With the addition of the graphite, these powders can fill the gaps between the steel wool, and as a consequence, the conductive paths increase so that the electrical resistivity of the composite continued to decrease. This hybrid addition of steel wool and graphite also solved the incomplete adhesion of steel wool and asphalt mastic in the mixture, as mentioned previously. Therefore, the addition of graphite is beneficial to the conductive network of steel wool, thus decreasing the optimum steel wool content. Meanwhile, because of this decrease of the steel wool content, there is no difficulty in the dispersion of steel wool.

Based on Fig. 11, effect of graphite content on the electrical resistivity of ECAM with 4% steel wool is shown in Fig. 12. It can be discovered that the electrical resistivity of ECAM-SG decreases greatly with the increasing graphite content from 10% to 15% and then decreases slowly with the graphite content. Therefore, the optimum graphite content of ECAM-SG is 15%.

The electrical resistivity values of different ECAMs are compared in Fig. 13. It can be observed that the electrical resistivity of ECAM-SG is only 35.4%, 14.8%, and 72% of that of ECAM-6%S, ECAM-15%G, and ECAM-20%G, respectively. Definitively, the hybrid addition of steel wool and graphite can indeed greatly improve the electrical conductivity of asphalt mixtures with a single conductive material.

Effect of Conductivity Materials on Pavement Properties of Asphalt Mixtures

According to the preceding analyses of the electrical conductivity of asphalt mixtures, the optimum mix proportions of ECAMs are obtained. ECAM-S, ECAM-G, and ECAM-SG involving 6% No. 4 steel wool, 15% graphite, and 4% No. 4 steel wool plus 15% graphite were fabricated in this section. However, dispersion of steel wool is a big problem when its content is 6%; thus, ECAM with 4% No. 4 steel wool is used for the following study about the pavement properties of ECAM-S and ECAM-SG. In addition, the plain asphalt mixture is used as a reference group in this part.

Moisture Susceptibility

Fig. 14 presents the results for the Marshall stability and RMS of ECAMs. As seen in Fig. 14, the ECAM-G has a slightly higher Marshall stability and lower immersion Marshall stability than AM. As a result, the RMS of ECAM-G is lower than that of AM, and the value cannot meet the basic requirement of asphalt mixtures (China DOT 2004). Other ECAMs can have equal RMS values compared with AM.

The unconditioned and conditioned splitting strength of ECAMs are shown in Fig. 15. As shown in Fig. 15, ECAM-G has nearly the same unconditioned splitting strength value as AM. However, the conditioned splitting strength of ECAM-G is lower

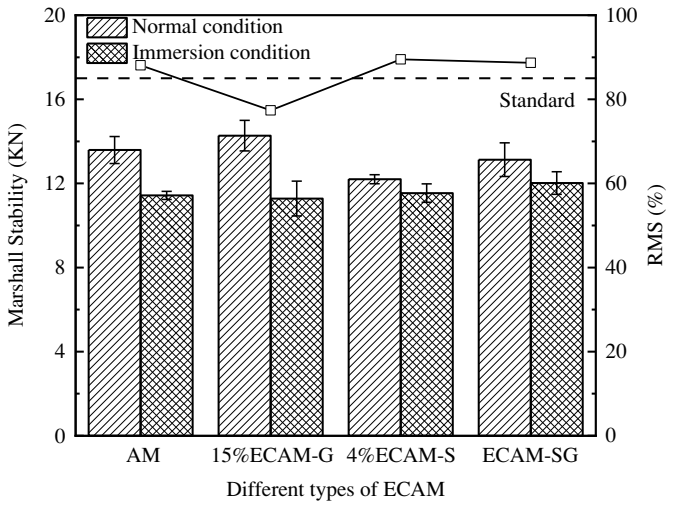

Fig. 14. Marshall stability and RMS of ECAMs.

J. Mater. Civ. Eng., 2022, 34(3): 04021466

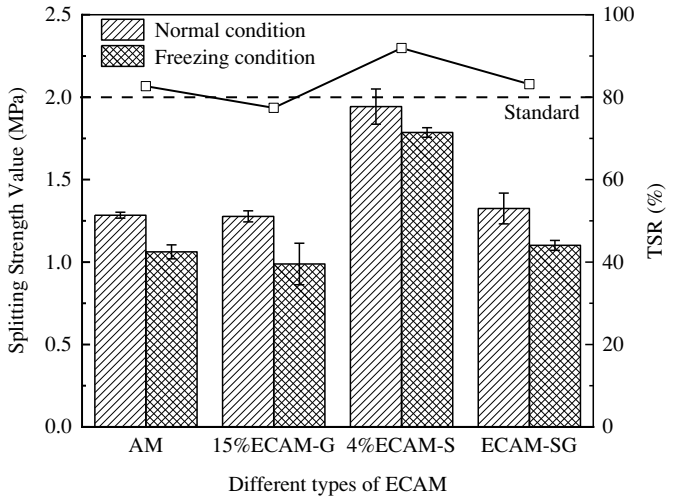

Fig. 15. Splitting strength value and TSR of ECAMs.

than that of AM so that ECAM-G has a lower TSR than AM. Meanwhile, the TSR of the ECAM-G also cannot reach the minimum requirement of asphalt mixtures (China DOT 2004). Unlike ECAM-G, the TSR of the ECAM-S exhibited an obvious advantage, being 11.19% higher than that of the plain asphalt mixture and 14.90% higher than that of the standard as shown in Fig. 15. It can be inferred that graphite and steel wool have a harmful and beneficial effect on the moisture susceptibility of asphalt mixtures, respectively. Combining the different effects of the two materials on the moisture susceptibility, the hybrid addition of steel wool and graphite has no harmful effect on the moisture susceptibility of asphalt mixtures, which is 1.01% higher than that of the plain asphalt mixture.

The results of both the immersion Marshall stability and freeze–thaw splitting tests indicate that graphite has negative effect on the moisture susceptibility of asphalt mixtures, whereas steel wool has positive effect on the moisture susceptibility. The strength theory of asphalt mixtures can be used to explain this phenomenon. The strength of an asphalt mixture is related to the cohesive and adhesive strength of asphalt mastic and the internal friction provided by the aggregate skeletal structure. In addition, the strength of asphalt mastic is more easily affected by moisture than the internal friction. Perhaps the adhesive interface between asphalt and graphite is more easily affected by moisture than that between asphalt and limestone powder. Thus, as micrometer particles, graphite can only affect the strength of asphalt mastic so that ECAM-G has a weak moisture susceptibility.

In contrast, as a centimeter fiber, steel wool can form a three-dimensional network structure in the mixture, thus greatly reinforcing the mixture and improving the internal friction between aggregates. This reinforcing effect on steel wool is little affected by moisture, so as to improve the moisture susceptibility of the asphalt mixture. This conclusion is consistent with the results of Hosseinian et al. (2020), who found that the Marshall stability of modified mixtures with steel wool additive increased with the increasing steel wool contents compared with the base sample.

Rutting Resistance

The dynamic stability of ECAMs is presented in Table 4. According to the results, the rutting resistance of AM can only reach the minimum requirement according to the Chinese specification (China DOT 2004). The dynamic stability of ECAM-S and

Table 4. Dynamic stability of ECAMs

Specimens	Dynamic stability (cycle/mm)
AM	872
ECAM-S	1,261
ECAM-G	3,693
ECAM-SG	5,887
Requirement	≥800

ECAM-G increased by 44.6% and 323.5% compared with AM, respectively. Besides, ECAM-SG has a very high dynamic stability, whereby the dynamic stability can increase to 5,887 cycle/mm combined with the advantages of steel wool and graphite. Therefore, it has been proved that ECAM-SG has an excellent rutting resistance, whose dynamic stability is far more than the requirement in the specification (China DOT 2004).

According to the results, definitively, both graphite and steel wool have a positive effect on the rutting resistance of asphalt mixture. This phenomenon can be explained as follows. For graphite, its specific surface area and the oil absorption are all higher than that of traditional limestone powder (Cheng et al. 2018). As a result, graphite has a high viscosity-increasing effect at high temperature compared with limestone powder, and this is why the asphalt mixture with graphite has an extremely high dynamic stability. This is consistent with the results of Rew et al (2017). In Rew et al.'s (2017) research, the complex shear modulus of the conductive asphalt mastic with graphite additive increases as the graphite content increases, which implies that graphite can improve rutting resistance of the composite. For steel wool, as mentioned previously, its three-dimensional network structure in the mixture can improve the internal friction between aggregates, thus improving the rutting resistance of asphalt mixture. Therefore, both steel wool and graphite can significantly improve the rutting resistance of the composite.

Low-Temperature Cracking Resistance

The flexural tensile strength and failure strain of ECAMs are shown in Fig. 16. It can be seen from Fig. 16 that graphite has little effect on the flexural tensile strength and failure strain of mixtures, which is very different from the steel wool. The results showed that the failure strain of ECAM-S is 89.02% higher than that of the plain asphalt mixture, as shown in Fig. 16(a). The flexural tensile strength also exhibited a similar growth trend as the failure strain, which is 72.37% higher than that of the plain asphalt mixture as shown in Fig. 16(b).

This phenomenon can be explained as follows. Compared with other materials in mixture, steel wool has excellent mechanical properties. Combined with its three-dimensional network structure in the mixture, steel wool can not only effectively reduce the uneven stress distribution inside the mixture, but also it significantly increases the tensile strength of the mixture. Consequently, steel wool can improve the tensile properties of asphalt mixture both in strength and deformability. Actually, this conclusion of steel wool on the cracking resistance is similar to that of other centimeter fibers, such as bagasse fiber (Li et al. 2020b) and basalt fiber (Cheng et al. 2018). As micrometer particles, graphite cannot improve the low-temperature cracking resistance of asphalt mixtures because it has no obvious reinforcing effect on mixture in tensile properties, and this conclusion can also be deduced in the freeze–thaw splitting test. Although steel wool exhibits a significant advantage in this property and graphite has no obvious disadvantage of that property, it is a pity that the hybrid addition of steel wool and graphite only slightly increases the failure strain of mixture and

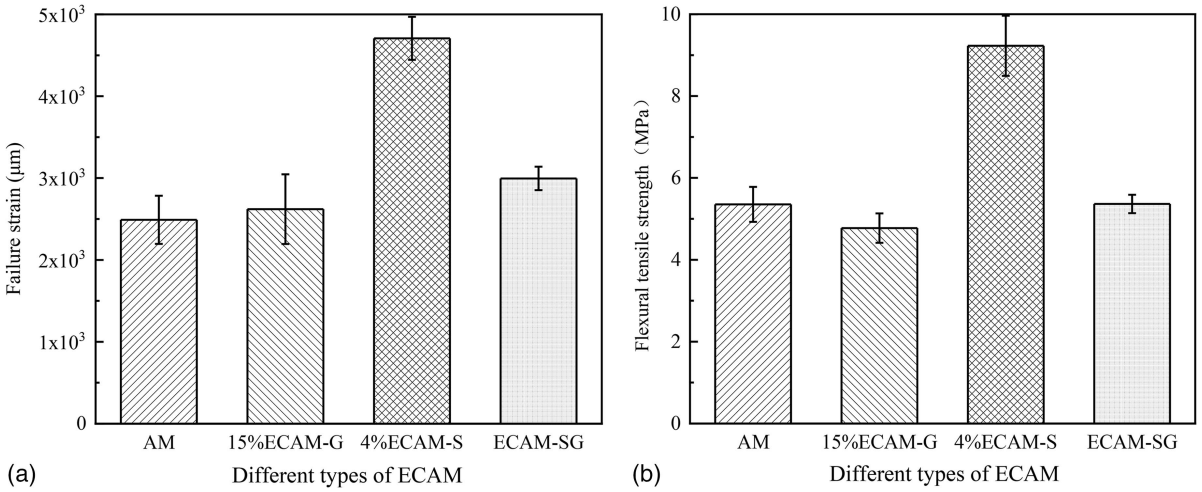

Fig. 16. (a) Failure strain; and (b) flexural tensile strength of the ECAMs.

slightly changes the flexural tensile strength of mixture, which highly degrades the positive of single addition of steel wool on the low-temperature cracking resistance of asphalt mixture. Perhaps the higher specific surface area and oil absorption capacity of graphite powder may reduce the interface friction between steel wool and asphalt matrix. Therefore, fiber slippage may occur more easily during the loading process. The accurate reason is unclear and should be further investigated.

Conclusions

Effects of steel wool and graphite on the electrical conductivity and pavement properties of asphalt mixture were studied to fabricate a better electrically conductive asphalt mixture. Based on the results and discussion, the following conclusions can be drawn:

- Steel wool with a larger diameter is more easily dispersed in asphalt mixtures due to the stiffness of this material, and it is greatly beneficial to improve the electrical conductivity of asphalt mixtures than that with a smaller diameter.
- In the optimum content, asphalt mixtures with steel wool exhibit a better electrical conductivity than that with graphite. However, steel wool at its optimum content is difficult to be well-dispersed in asphalt mixture. To solve the dispersion problem and ensure the electrical conductivity, the hybrid addition of steel wool and graphite into asphalt mixtures is employed. Results show that the hybrid addition method not only can reduce the steel wool content to avoid the dispersion problem, but also it further improves the electrical conductivity of asphalt mixtures.
- Graphite has a high viscosity-increasing effect at high temperature, but the adhesive interface between asphalt and graphite is more easily affected by moisture. Thus, asphalt mixtures with graphite have a much higher rutting resistance but a poor moisture susceptibility than that of the plain asphalt mixture. Besides, steel wool has a reinforcing effect on the tensile properties of asphalt mixture due to its three-dimensional network structure in mixture. As a result, compared with the plain asphalt mixture, the failure strain and flexural strength of asphalt mixtures with steel wool can increased by 89.02% and 72.37%, respectively. Besides, asphalt mixture with steel wool can have a slightly higher moisture susceptibility and rutting resistance than the plain asphalt mixture. Combining the different effects of steel wool and graphite, asphalt mixtures with steel wool and graphite have excellent rutting resistance and good moisture susceptibility and low-temperature cracking resistance.
- To fabricate a uniform and highly electrically conductive asphalt mixture with better pavement properties, it is recommended that the hybrid addition of 15% graphite and 4% steel wool is employed into asphalt mixture, which is more suitable for fabricating intelligent materials.

Future Work

This work only focused on the fabrication of a pavement material with good electrical conductivity and pavement properties, but the corrosion of steel wool was not considered, which may cause distress to the asphalt mixture. Therefore, use of stainless steel wool or other noncorrosive conductive fibers instead of steel wool will be studied in the future. Besides, the single addition of steel wool shows significant advantages in low-temperature cracking resistance. It is still unclear why the hybrid addition of steel wool and graphite only slightly increases the failure strain of mixture and causes little change in the flexural tensile strength of mixture, which remains to be investigated further.

Data Availability Statement

Some or all data, models, or code that support the findings of this study are available from the corresponding author upon reasonable request.

Acknowledgments

The authors thank the research funds from the National Key R&D Program of China (2018YFB1600100), the Natural Science Foundation of Liaoning Province (2020-MS-116), and Natural Science Foundation of Hunan Province (2019JJ40093).

References

Ameri, M., S. Nowbakht, M. Molayem, and M. R. M. Aliha. 2016. "Investigation of fatigue and fracture properties of asphalt mixtures modified with carbon nanotubes." *Fatigue Fract. Eng. Mater. Struct.* 39 (7): 896–906. https://doi.org/10.1111/ffe.12408.

Cheng, Y., D. Yu, Y. Gong, C. Zhu, J. Tao, and W. Wang. 2018. "Laboratory evaluation on performance of eco-friendly basalt fiber and diatomite compound modified asphalt mixture." *Materials* 11 (12): 2400. https://doi.org/10.3390/ma11122400.

China DOT. 2004. *Technical specification for construction of highway asphalt pavements*. JTG F40-2004. Beijing: China DOT.

China DOT. 2011. *Standard test methods of bitumen and bituminous mixtures for highway engineering*. JTG E20-2011. Beijing: China DOT.

Faßbender, S., and M. Oeser. 2020. "Investigation on an absorbing layer suitable for a noise-reducing two-layer pavement." *Materials* 13 (5): 1–19. https://doi.org/10.3390/ma13051235.

García, A., E. Schlangen, M. Ven, and Q. Liu. 2009. "Electrical conductivity of asphalt mortar containing conductive fibers and fillers." *Constr. Build. Mater.* 23 (10): 3175–3181. https://doi.org/10.1016/j.conbuildmat.2009.06.014.

Guo, Q., H. Wang, Y. Gao, Y. Jiao, F. Liu, and Z. Dong. 2020. "Investigation of the low-temperature properties and cracking resistance of fiber-reinforced asphalt concrete using the DIC technique." *Eng. Fract. Mech.* 229 (Apr): 106951. https://doi.org/10.1016/j.engfracmech.2020.106951.

Ha, J., S. Hong, J. Ryu, J. Bae, and S. Park. 2019. "Development of multifunctional graphenepolymer composites having electromagnetic interference shielding and deicing properties." *Polymers* 11 (12): 2101. https://doi.org/10.3390/polym11122101.

Han, B., B. Han, and J. Ou. 2009. "Experimental study on use of nickel powder-filled portland cement-based composite for fabrication of piezoresistive sensors with high sensitivity." *Sens. Actuators, A* 149 (1): 51–55. https://doi.org/10.1016/j.sna.2008.10.001.

Han, B., K. Zhang, T. Burnham, E. Kwon, and X. Yu. 2013. "Integration and road tests of a self-sensing CNT concrete pavement system for traffic detection." *Smart Mater. Struct.* 22 (1): 015020. https://doi.org/10.1088/0964-1726/22/1/015020.

Hasni, H., A. H. Alavi, K. Chatti, and N. Lajnef. 2017. "A self-powered surface sensing approach for detection of bottom-up cracking in asphalt concrete pavements: Theoretical/numerical modeling." *Constr. Build. Mater.* 144 (Jul): 728–746. https://doi.org/10.1016/j.conbuildmat.2017.03.197.

Hosseinian, S. M., V. Najafi Moghaddam Gilani, P. Mehraban Joobani, and M. Arabani. 2020. "Investigation of moisture sensitivity and conductivity properties of inductive asphalt mixtures containing steel wool fiber." *Adv. Civ. Eng.* 2020: 8890814. https://doi.org/10.1155/2020/8890814.

Jolliffe, B. W., R. P. Tye, and R. W. Powell. 1966. "The thermal and electrical conductivities of scandium, yttrium and manganese and twelve rare-earth metals, at normal temperature." *J. Less-Common Met.* 11 (6): 388–394. https://doi.org/10.1016/0022-5088(66)90084-1.

Li, C., T. Yuan, H. Zheng, and S. Wang. 2017. "Study on pavement performance of thermal conductive asphalt concrete used in electric melting snow road." *Urban Roads Bridges Flood Control* 1009–7716. https://doi.org/10.16799/j.cnki.csdqyfh.2017.04.054.

Li, M., G. Wu, E. H. Fini, M. Yu, and Z. Xu. 2020a. "Investigating the healing capacity of asphalt mixtures containing iron slag." *Constr. Build. Mater.* 261 (Nov): 119446. https://doi.org/10.1016/j.conbuildmat.2020.119446.

Li, Z., X. Zhang, C. Fa, Y. Zhang, J. Xiong, and H. Chen. 2020b. "Investigation on characteristics and properties of bagasse fibers: Performances of asphalt mixtures with bagasse fibers." *Constr. Build. Mater.* 248 (Jul): 118648. https://doi.org/10.1016/j.conbuildmat.2020.118648.

Moreno-Navarro, F., M. Sol-Sánchez, F. Gámiz, and M. C. Rubio-Gámez. 2018. "Mechanical and thermal properties of graphene modified asphalt binders." *Constr. Build. Mater.* 180 (Aug): 265–274. https://doi.org/10.1016/j.conbuildmat.2018.05.259.

Na, W. 2019. "History data free piezoelectric based non-destructive testing technique for debonding detection of composite structures." *Compos. Struct.* 226 (Jul): 111225. https://doi.org/10.1016/j.compstruct.2019.111225.

Na, W., and J. Baek. 2019. "Piezoelectric impedance-based non-destructive testing method for possible identification of composite debonding depth." *Micromachines* 10 (9): 621. https://doi.org/10.3390/mi10090621.

Norambuena-Contreras, J., and A. Garcia. 2016. "Self-healing of asphalt mixture by microwave and induction heating." *Mater. Des.* 106 (Sep): 404–414. https://doi.org/10.1016/j.matdes.2016.05.095.

Norambuena-Contreras, J., E. Yalcin, A. Garcia, T. Al-Mansoori, M. Yilmaz, and R. Hudson-Griffiths. 2018. "Effect of mixing and ageing on the mechanical and self-healing properties of asphalt mixtures containing polymeric capsules." *Constr. Build. Mater.* 175 (Jun): 254–266. https://doi.org/10.1016/j.conbuildmat.2018.04.153.

Ou, J., and B. Han. 2009. "Piezoresistive cement-based strain sensors and self-sensing concrete components." *J. Intell. Mater. Syst. Struct.* 20 (3): 329–336. https://doi.org/10.1177/1045389X08094190.

Rao, R., J. Fu, Y. Chan, C. Y. Tuan, and C. Liu. 2018. "Steel fiber confined graphite concrete for pavement deicing." *Composites, Part B* 155 (Jun): 187–196. https://doi.org/10.1016/j.compositesb.2018.08.013.

Rew, Y., A. Baranikumar, A. V. Tamashausky, S. El-Tawil, and P. Park. 2017. "Electrical and mechanical properties of asphaltic composites containing carbon based fillers." *Constr. Build. Mater.* 135 (Mar): 394–404. https://doi.org/10.1016/j.conbuildmat.2016.12.221.

Shen, A., H. Wu, X. Yang, Z. He, and J. Meng. 2020. "Effect of different fibers on pavement performance of asphalt mixture containing steel slag." *J. Mater. Civ. Eng.* 32 (11): 04020333. https://doi.org/10.1061/(ASCE)MT.1943-5533.0003427.

Sun, Y., S. Wu, Q. Liu, W. Zeng, Z. Chen, Q. Ye, and P. Pan. 2017. "Self-healing performance of asphalt mixtures through heating fibers or aggregate." *Constr. Build. Mater.* 150 (Sep): 673–680. https://doi.org/10.1016/j.conbuildmat.2017.06.007.

Wang, L., H. Wang, Q. Zhao, H. Yang, H. Zhao, and B. Huang. 2019. "Development and prospect of intelligent pavement." *China J. Highway Transp.* 32 (4): 50–72. https://doi.org/10.19721/j.cnki.1001-7372.2019.04.004.

Wang, Z., Q. Dai, P. David, and Z. You. 2016. "Investigation of microwave healing performance of electrically conductive carbon fiber modified asphalt mixture beams." *Constr. Build. Mater.* 126 (Nov): 1012–1019. https://doi.org/10.1016/j.conbuildmat.2016.09.039.

Wu, J., J. Liu, and F. Yang. 2015. "Three-phase composite conductive concrete for pavement deicing." *Constr. Build. Mater.* 75 (Jan): 129–135. https://doi.org/10.1016/j.conbuildmat.2014.11.004.

Wu, S. P., L. T. Mo, and Z. H. Shui. 2003. "Piezoresistivity of graphite modified asphalt-based composites." *Key Eng. Mater.* 249 (1662–9795): 391–396. https://doi.org/10.4028/www.scientific.net/KEM.249.391.

Xin, X., M. Liang, Z. Yao, L. Su, J. Zhang, P. Li, C. Sun, and H. Jiang. 2020. "Self-sensing behavior and mechanical properties of carbon nanotubes/epoxy resin composite for asphalt pavement strain monitoring." *Constr. Build. Mater.* 257 (Oct): 119404. https://doi.org/10.1016/j.conbuildmat.2020.119404.

Ye, H., X. Wang, N. Fang, and X. Nin. 2019. "Road deicing technology with microwave heating in winter." *Eng. J. Wuhan Univ.* 52 (11): 981–988. https://doi.org/10.14188/j.1671-8844.2019-11-006.

Zhang, Q., Y. Yu, W. Chen, T. Chen, Y. Zhou, and H. Li. 2016. "Outdoor experiment of flexible sandwiched graphite-PET sheets based self-snow-thawing pavement." *Cold Reg. Sci. Technol.* 122 (Feb): 10–17. https://doi.org/10.1016/j.coldregions.2015.10.016.